PHYSICAL REVIEW
LETTERS

VOLUME 86 16 APRIL 2001 NUMBER 16

Bose-Einstein Condensation of Metastable Helium

F. Pereira Dos Santos, J. Léonard, Junmin Wang,* C. J. Barrelet, F. Perales,† E. Rasel,‡
C. S. Unnikrishnan,§ M. Leduc, and C. Cohen-Tannoudji

Collège de France, Laboratoire Kastler Brossel, Département de Physique, Ecole Normale Supérieure, 24 rue Lhomond, 75231 Paris Cedex 05, France

(Received 19 March 2001)

We have observed a Bose-Einstein condensate in a dilute gas of ^{4}He in the 2^3S_1 metastable state. We find a critical temperature of $(4.7 \pm 0.5)\ \mu$K and a typical number of atoms at the threshold of 8×10^6. The maximum number of atoms in our condensate is about 5×10^5. An approximate value for the scattering length $a = (16 \pm 8)$ nm is measured. The mean elastic collision rate at threshold is then estimated to be about $2 \times 10^4\ s^{-1}$, indicating that we are deeply in the hydrodynamic regime. The typical decay time of the condensate is 2 s, which places an upper bound on the rate constants for two-body and three-body inelastic collisions.

DOI: 10.1103/PhysRevLett.86.3459 PACS numbers: 03.75.Fi, 05.30.Jp, 32.80.Pj

Bose-Einstein condensation (BEC) of dilute atomic gases was first observed in alkali atoms in 1995 and then, a few years later, in atomic hydrogen. Since then, the field has developed in a spectacular way both experimentally and theoretically [1]. So far only condensates with atoms in their electronic ground state have been produced.

Several laboratories are currently involved in the search for BEC of atoms in an excited state, namely, noble gases in an excited metastable state. Helium in its triplet metastable 2^3S_1 state (^{4}He*) is of particular interest. The first advantage of ^{4}He* is its large internal energy (19.8 eV). It allows for very efficient detection of the atom by ionization after collision with another atom or a surface, which can be of interest for atomic lithography [2,3]. Second, helium is a relatively simple atom which allows for quasi-exact calculations that are useful in metrological applications. Third, mixtures of ^{3}He and ^{4}He can be used to study quantum degenerate mixtures of bosons and fermions. Finally, Penning collisions are expected to be inhibited for spin polarized atoms due to spin selection rules. This effect, first pointed out in [4], was confirmed by subsequent calculations [5].

The present Letter describes the observation of BEC of ^{4}He* atoms. Similar results have also been obtained at IOTA, Orsay [6]. The two experiments differ by their detection methods. The IOTA group detects the atoms falling on a microchannel plate, whereas we use an optical absorption imaging of the atomic cloud on a charge-coupled device (CCD) camera. The two experiments therefore give different and complementary information on the physics of BEC in ^{4}He*.

The first step of our experiment is the efficient loading of a magneto-optical trap (MOT). The experimental setup is described in detail in [7]. A discharge atomic source ensures a high flux of triplet metastable atoms of 10^{14} atoms/s.sr, with a mean velocity of about 1000 m/s. The atomic beam is collimated [8] and Zeeman slowed by laser light at 1083 nm (2^3S_1-2^3P_2 transition). A narrow frequency band master oscillator (distributed Bragg reflector diode laser) injects a Yb-doped fiber amplifier with an output power of 500 mW. Using this setup, it is possible to trap $\sim 8 \times 10^8$ atoms in the MOT at a temperature of 1 mK.

^{4}He* atoms are confined at the center of a small ($4 \times 4 \times 5$ cm) quartz cell. All coils are external to the cell (see Fig. 1). Coils Q_1 and Q_2 (144 turns and 7 cm diameter) combined with coil C_3 (108 turns and 4 cm diameter) produce an anisotropic magnetic Ioffe-Pritchard trap. Two additional Helmholtz coils reduce the bias field, in order to increase the radial confinement of the trap. A current of 45 A in all the coils produces a 4.2 G bias field, radial gradients of 280 G/cm, and an axial curvature of 200 G/cm^2.

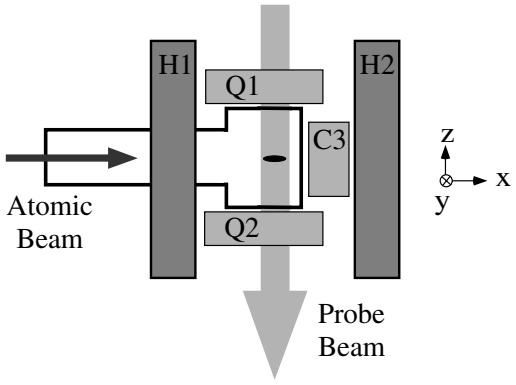

FIG. 1. Top view of the magnetic trap. Coils Q_1 and Q_2 produce a quadrupole field used for the MOT. Combined with a third coil C_3, they produce a magnetic Ioffe-Pritchard trap. Helmholtz coils H_1 and H_2 compensate the bias field. The probe beam used for optical detection is perpendicular to the longitudinal axis of the trap.

These values correspond to trapping frequencies of 115 Hz in the axial and 1090 Hz in the radial directions. The current in the coils can be switched off in 200 μs.

The second step of the experiment is the loading of the magnetic trap. After switching off the MOT field, the cloud is further cooled down to about 300 μK during a 1 ms optical molasses phase. To increase the transfer efficiency from the molasses to the magnetic trap, the atoms are optically pumped by a circularly polarized laser pulse. 3×10^8 atoms are loaded in the magnetic trap. The lifetime of the atomic cloud in the magnetic trap is about 35 s, and its temperature is 1.2 mK after compression and bias compensation.

The last step of the experiment consists of evaporative cooling performed by radio frequency (rf) induced spin flips. The frequency is ramped down from 160 MHz to around 12 MHz in 15 s. After evaporation, the trap is switched off and the cloud released from the trap is probed by absorption imaging on a CCD camera whose quantum efficiency is 1.5% at 1083 nm.

When the rf frequency of the evaporation is ramped down to a final frequency below 13 MHz, a narrow structure appears on the absorption image which we identify as a condensate. The strongest evidence for the presence of the condensate is the evolution of the shape of this structure when released from the trap in the time-of-flight (TOF) measurement. Its ellipticity increases as the expansion time is increased, and its anisotropy undergoes an inversion (see Fig. 2a). This observation is a consequence of the mean-field interaction between atoms in the condensate [9]. The theoretical prediction containing no adjustable parameters agrees well with our measurements (see Fig. 2b).

The spatial distribution of the absorption pictures is fitted with the sum of two functions, one for the condensate and one for the thermal cloud (see inset in Fig. 3). The function for the condensate is an integration along the z axis of a paraboloidal distribution. It describes the equilibrium density profile of the condensate within the harmonic trap in the Thomas-Fermi limit [10]. The function for the thermal cloud is a g_2 function valid for a bosonic gas close to the transition where the chemical potential μ is an adjustable parameter [1]. From the fit, we extract the ratio between the number of atoms in the condensate, N_0, and the total number of atoms, N. Plotting N_0/N versus the temperature T (Fig. 3) gives the value of the critical temperature $T_c = (4.7 \pm 0.5)$ μK, which is confirmed by a TOF measurement performed on a thermal cloud just above the transition.

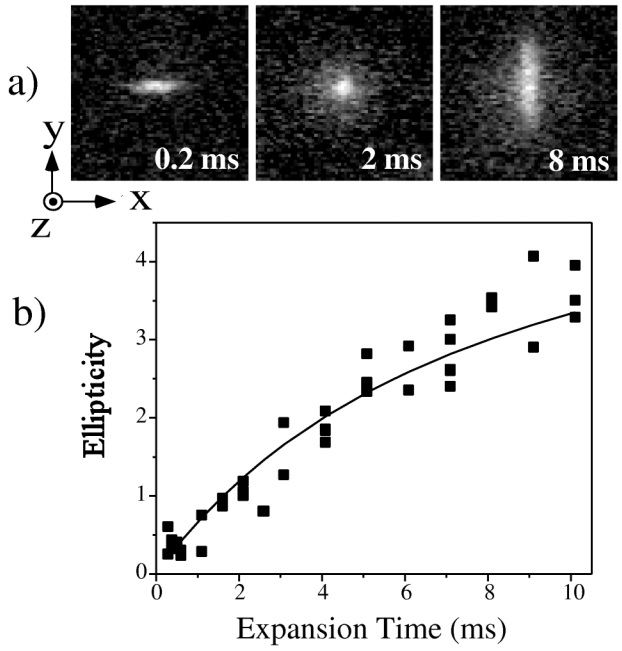

FIG. 2. (a) Time-of-flight absorption images (1.4 × 1.4 mm) after an expansion time of 0.2, 2, and 8 ms; (b) ellipticity of the condensate for increasing expansion times. The solid line is the theoretical prediction without any adjustable parameters. The inversion of ellipticity is characteristic of the behavior of an expanding condensate.

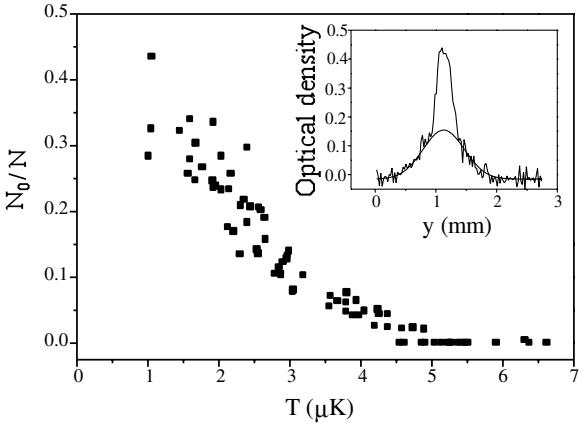

FIG. 3. Condensed fraction N_0/N versus T. The inset shows a 1D profile of an absorption image, displaying a bimodal structure, composed of a condensate and a thermal component, which is characteristic of the bosonic gas below T_c. The thermal component is fitted for clarity.

The results presented until now are based only on measured sizes of the clouds and on relative numbers like N_0/N which do not require absolute calibration of the optical detection. The procedure described previously for the measurement of ellipticity and critical temperature is not suitable for absolute measurements of N and N_0. So, we use a different procedure to calibrate the number of atoms at threshold. The current is switched off in two steps: first, in the Helmholtz coils, then, after a delay of 10 ms, in the three coils Q_1, Q_2, and C_3, whereas the current in all five coils was switched off simultaneously for the measurements above. Then, we take an absorption image with an exposure time $T_{\text{exp}} = 200$ μs after a TOF time of 5 ms. This procedure minimizes the effects of eddy currents of the Helmholtz coils which last several milliseconds, Zeeman shifting the atomic resonance with respect to the probe beam frequency [11]. There are two other obvious sources of sensitivity losses. First, the width of the absorption line shape is measured to be twice the natural linewidth, which we attribute to laser linewidth and power broadening. This reduces the absorption cross section by a factor of 2. Second, the probe beam propagates perpendicularly to the x axis of the Ioffe-Pritchard trap (see Fig. 1) along which atoms are polarized. It would therefore be necessary to take into account the populations of the different Zeeman sublevels, and the Clebsch-Gordan coefficients of the various Zeeman optical transitions excited by the probe beam. But any residual magnetic field redistributes the populations among Zeeman sublevels. Assuming equally populated sublevels increases the loss by a factor of $9/5$. Finally, there is another source of losses which is specific to $^4\text{He}^*$ when optically detected and particularly important at the high densities obtained in our experiment. The metastable atoms have a huge Penning ionization cross section in the presence of resonant light, so that losses can accumulate during the probe pulse at large densities. Unfortunately, probing at low intensity is no longer possible if T_{exp} is made shorter because of the low efficiency of the CCD camera. This long exposure time also increases the acceleration of the atoms due to radiation pressure which pushes them out of resonance [12]. In the present stage of the experiment, it is difficult to give a quantitative description of the combined effect of these phenomena. So, we prefer to wait an expansion time of 5 ms to sufficiently reduce the atomic density. Indeed, we observe that the measured number of atoms is an increasing function of the expansion time reaching a plateau after 5–6 ms. After the corrections mentioned above, the total number of atoms N_c at the threshold is measured to be 5×10^6 atoms with an accuracy of about 50%.

N_c can also be estimated from $N_c = 1.202(k_B T_c/\hbar\bar{\omega})^3$, where $\bar{\omega}$ is the geometrical average of the frequencies of the trap [13]. We deduce $N_c = 8.2 \times 10^6$ atoms with an uncertainty of about 30% compatible with the previous value. Because it is easier to trace down the error on N_c when derived from T_c, we arbitrarily choose this value of N_c to estimate the scattering length a. Also, assuming that the transition occurs at a phase space density equal to $n(0)\lambda_{dB}^3 = 2.612$, where λ_{dB} is the de Broglie wavelength, we can also derive the density at the center of the trap $n(0) = (3.8 \pm 0.7) \times 10^{13}$ atoms/cm^3 at the transition.

Within the Thomas-Fermi approximation, one can extract the chemical potential μ from the size of the condensate [10]. As the optical detection around the transition has been calibrated, we can now use our previous relative measurements to deduce the absolute number of condensed atoms N_0 below the transition. Typical values of $\mu = 1.4 \times 10^{-29}$ J and $N_0 = (4 \pm 1.5) \times 10^5$ are obtained with condensates prepared at temperatures ranging from 1.2 to 3 μK. Finally, an estimation of the scattering length a can be given using $a = \sigma/15N_0 \times (2\mu/\hbar\bar{\omega})^{5/2}$, where $\sigma = (\hbar/m\bar{\omega})^{1/2}$ is the characteristic size of the ground state of the trap. We find $a = (16 \pm 8)$ nm which is compatible with the value given by recent theoretical works [5,14]. The error is mostly due to the uncertainty on the number of atoms. Knowing the scattering length a, the density at the center of the trap $n(0)$, and the critical temperature T_c, we obtain a mean rate of elastic collisions $\bar{\gamma}_{\text{coll}} \simeq 2 \times 10^4$ s^{-1} near threshold, leading to $\bar{\omega}/\bar{\gamma}_{\text{coll}} = 0.17$. We thus enter in the hydrodynamic regime, an interesting feature for a gas above T_c [15–18].

Figure 4 shows the evolution of the number of atoms in the condensate versus the trapping time. The typical lifetime is about 2 s. In the present stage of the experiment, it is not possible to discriminate between two-body and three-body decay. However, assuming that only two-body collisions lead to losses in the condensate, we can place an upper bound on the collision rate constant G between spin polarized $^4\text{He}^*$ atoms, which is predicted to be inhibited by a factor of 10^4 compared with the rate constant for Penning ionization collisions between unpolarized atoms. The evolution equation of the number of atoms $\dot{N}(t) = -G \int n^2(\mathbf{r})\, d^3r$, integrated on the whole condensate in the Thomas-Fermi approximation, gives the evolution of the number of atoms N_0 in the condensate. A fit leads to $G \leq (4.2 \pm 0.6) \times 10^{-14}$ cm^3/s, which corresponds to a

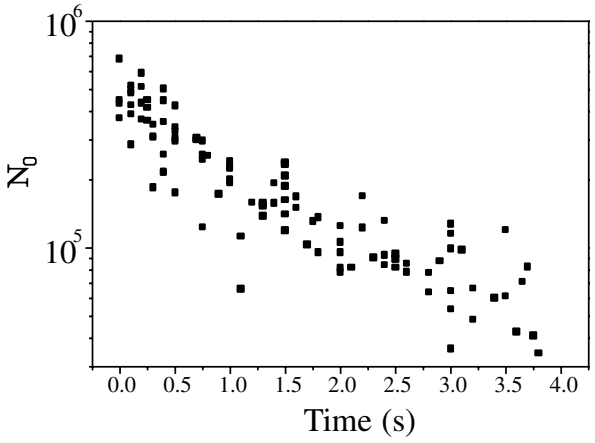

FIG. 4. Decay of the condensate. This measurement was performed with an rf shield at 12.3 MHz.

reduction factor larger than 2×10^3, much larger than the previously measured ones [19,20], in agreement with theoretical calculations [4,5].

If one assumes now that three-body collisions are responsible for the decay of N_0, one can as well give an upper bound for the rate constant L defined by $\dot{N}(t) = -L \int n^3(\mathbf{r})\, d^3r$. Fitting our data gives $L \leq (2.8 \pm 0.2) \times 10^{-27}$ cm^6/s. This value can be compared to theoretical predictions [21,22]: for example, our upper limit is compatible with [21], which finds $L = 3.9\hbar a^4/2m = 2 \times 10^{-27}$ cm^6/s.

In conclusion, this Letter shows the evidence for the formation of a BEC of helium atoms in the metastable state 2^3S_1. Our results concerning the losses due to inelastic collisions show that the spin polarization does inhibit the Penning ionization collisions between two metastable helium atoms by more than 3 orders of magnitude, as theoretically predicted. We find a large scattering length, which results in very large rates of elastic collisions: the cold gas at threshold is in the hydrodynamic regime, which we plan to study in more detail. We also plan to exploit further the original characteristics of this newborn condensate of atoms in an excited state.

The authors thank J. Dalibard, C. Salomon, D. Guéry-Odelin, and Y. Castin for helpful discussions and careful reading of the manuscript and F. Pavone and A. Sinatra-Castin for their contribution in the early stages of the experiment. We thank the IOTA group in Orsay for communicating their preliminary results as soon as they were obtained, which was a great stimulation for our group achieving helium BEC eight days later. Also, we thank M. Roux for the loan of the Hamamatsu CCD camera (C4880-30) with which the BEC was first detected in our group. C. J. B. acknowledges support from the Schweizerische Studienstiftung. Laboratoire Kastler Brossel is Unité de Recherche de l'Ecole Normale Supérieure et de l'Université Pierre et Marie Curie, associée au CNRS (UMR 8552).

*Permanent address: Institute of Opto-Electronics, Shanxi University, 36 Wucheng Road, Taiyuan, Shanxi 030006, China.

†Permanent address: Laboratoire de Physique des Lasers, UMR 7538 du CNRS, Université Paris Nord, Avenue J. B. Clément, 93430 Villetaneuse, France.

‡Present address: Universität Hannover, Welfengarten 1, D-30167 Hannover, Germany.

§Permanent address: TIFR, Homi Bhabha Road, Mumbai 400005, India.

[1] For an overview on the subject, see, for example, *Proceedings of the International School of Physics "Enrico Fermi,"* Course CXL, edited by M. Inguscio, S. Stringari, and C. E. Wieman (IOS Press, Amsterdam, 1999).

[2] A. Bard, K. K. Berggren, J. L. Wilbur, J. D. Gillaspy, S. L. Rolston, J. J. McClelland, W. D. Phillips, M. Prentiss, and G. M. Whitesides, J. Vac. Sci. Technol. B **15**, 1805 (1997).

[3] S. Nowak, T. Pfau, and J. Mlynek, Appl. Phys. B **63**, 203 (1996).

[4] G. V. Shlyapnikov, J. T. M. Walraven, U. M. Rahmanov, and M. W. Reynolds, Phys. Rev. Lett. **73**, 3247 (1994).

[5] P. O. Fedichev, M. W. Reynolds, U. M. Rahmanov, and G. V. Shlyapnikov, Phys. Rev. A **53**, 1447 (1996); V. Venturi, I. B. Whittingham, P. J. Leo, and G. Peach, Phys. Rev. A **60**, 4635 (1999).

[6] A. Robert, O. Sirjean, A. Browaeys, J. Poupard, S. Nowak, D. Boiron, C. I. Westbrook, and A. Aspect, Sci. Mag. (to be published).

[7] F. Pereira Dos Santos, F. Perales, J. Léonard, A. Sinatra, Junmin Wang, F. S. Pavone, E. Rasel, C. S. Unnikrishnan, and M. Leduc, Eur. Phys. J. Appl. Phys. (to be published), e-print arXiv:physics/0103064.

[8] E. Rasel, F. Pereira Dos Santos, F. S. Pavone, F. Perales, C. S. Unnikrishnan, and M. Leduc, Eur. Phys. J. D **7**, 311 (1999).

[9] Y. Castin and R. Dum, Phys. Rev. Lett. **77**, 5315 (1996).

[10] See, for example, F. Dalfovo, S. Giorgini, L. P. Pitaevskii, and S. Stringari, Rev. Mod. Phys. **71**, 463 (1999).

[11] Because of the large size of the Helmholtz coils, one can, however, neglect the spatial gradients of magnetic fields produced by eddy currents. The measurement of the sizes and of the ratios N_0/N is thus not affected by these remaining magnetic fields.

[12] Actually, we use a standing wave made of two independent opposite beams in order to reduce the effect of radiation pressure.

[13] This formula is valid only in the case of an ideal bosonic gas and does not require any further assumption. Effects due to mean field have been calculated for a harmonic trap [23] and effects due to quantum correlations have been calculated in a box [24]. The shift of the critical temperature T_c can be quite large ($\delta T_c/T_c \simeq 15\%$) for both of these effects, due to the large value of the scattering length a, but have opposite signs. It would be interesting to study them both in more detail for a harmonic trap.

[14] V. Venturi and I. B. Whittingham, Phys. Rev. A **61**, 060703R (2000); P. J. Leo, V. Venturi, I. B. Whittingham, and J. F. Babb, e-print arXiv:physics/0011072.

[15] D. M. Stamper-Kurn, H.-J. Miesner, S. Inouye, M. R. Andrews, and W. Ketterle, Phys. Rev. Lett. **81**, 500 (1998).

[16] A. Griffin, Wen-Chin Wu, and S. Stringari, Phys. Rev. Lett. **78**, 1838 (1997).

[17] D. Guéry-Odelin, F. Zambelli, J. Dalibard, and S. Stringari, Phys. Rev. A **60**, 4851 (1999).

[18] H. Wu and E. Arimondo, Phys. Rev. A **58**, 3822 (1998).

[19] N. Herschbach, P. J. J. Tol, W. Hogervorst, and W. Vassen, Phys. Rev. A **61**, 050702R (2000).

[20] S. Nowak, A. Browaeys, J. Poupard, A. Robert, D. Boiron, C. Westbrook, and A. Aspect, Appl. Phys. B **70**, 455 (2000).

[21] P. O. Fedichev, M. W. Reynolds, and G. V. Shlyapnikov, Phys. Rev. Lett. **77**, 2921 (1996).

[22] B. P. Esry, C. H. Greene, and J. P. Burke, Phys. Rev. Lett. **83**, 1751 (1999).

[23] S. Giorgini, L. P. Pitaevskii, and S. Stringari, Phys. Rev. A **54**, R4633 (1996).

[24] G. Baym, J.-P. Blaizot, M. Holzmann, F. Laloë, and D. Vautherin, Phys. Rev. Lett. **83**, 1703 (1999).